

See discussions, stats, and author profiles for this publication at: <https://www.researchgate.net/publication/7746435>

Adsorption of Water on Reconstructed Rutile TiO₂ (011)-(2×1): TiO Double Bonds and Surface Reactivity

ARTICLE *in* JOURNAL OF THE AMERICAN CHEMICAL SOCIETY · AUGUST 2005

Impact Factor: 12.11 · DOI: 10.1021/ja0511624 · Source: PubMed

CITATIONS

70

READS

91

8 AUTHORS, INCLUDING:



Antonio Tilocca

University College London

79 PUBLICATIONS 2,164 CITATIONS

SEE PROFILE



Annabella Selloni

Princeton University

149 PUBLICATIONS 11,213 CITATIONS

SEE PROFILE



Thomas J Beck

Novelis Inc.

9 PUBLICATIONS 411 CITATIONS

SEE PROFILE



Matthias Batzill

University of South Florida

116 PUBLICATIONS 4,341 CITATIONS

SEE PROFILE

J|A|C|S

A R T I C L E S

Published on Web 00/00/0000

Adsorption of Water on Reconstructed Rutile $\text{TiO}_2(011)-(2 \times 1)$: Ti=O Double Bonds and Surface Reactivity

Cristiana Di Valentin,^{†,‡} Antonio Tilocca,[‡] Annabella Selloni,^{*,‡} T. J. Beck,[§]
Andreas Klust,[§] Matthias Batzill,[§] Yaroslav Losovj,^{⊥,||} and Ulrike Diebold^{*,§}

Contribution from the Dipartimento di Scienza dei Materiali, Università degli Studi di Milano-Bicocca, 20125 Milano, Italy, Department of Chemistry, Princeton University, Princeton, New Jersey 08540, Department of Physics, Tulane University, New Orleans, Louisiana 70118, Center for Advanced Microstructures and Devices, Louisiana State University, Baton Rouge, Louisiana 70806, and Department of Physics and Astronomy and the Center for Material Research and Analysis, University of Nebraska, Lincoln, Nebraska 68588

Received February 23, 2005; E-mail: aselloni@princeton.edu; diebold@tulane.edu

Abstract: Recent combined experimental and theoretical studies (Beck et al., *Phys. Rev. Lett.* **2004**, 93, 036104) have provided evidence for Ti=O double-bonded titanyl groups on the reconstructed rutile $\text{TiO}_2(011)-(2 \times 1)$ surface. The adsorption of water on the same surface is now investigated to further probe the properties of these groups, as well as to confirm their existence. Ultraviolet photoemission experiments show that water is adsorbed in molecular form at a sample temperature of 110 K. At the same time, the presence of a 3σ state in the photoemission spectra and work function measurements indicate a significant amount of hydroxyls within the first monolayer of water. At room temperature, scanning tunneling microscopy (STM) suggests that dissociated water is present, and about 30 of the surface active sites are hydroxylated. These findings are well explained by total energy density functional theory calculations and Car–Parrinello molecular dynamics simulations for water adsorption on the titanyl model of $\text{TiO}_2(011)-(2 \times 1)$. The theoretical results show that a mixed molecular/dissociative layer is the most stable configuration in the monolayer regime at low temperatures, while complete dissociation takes place at 250 K. The arrangement of the protonated mono-coordinated oxygens in the mixed molecular/dissociated layer is consistent with the observed short-range order of the hydroxyls in the STM images.

1. Introduction

The interaction of water with solid surfaces is of great interest for both basic sciences and applications.^{1–4} Water affects everything in the ambient environment; thus, the surface chemistry of water has a great influence in many areas such as corrosion, passivation, and heterogeneous catalysis. In particular, the discovery of photochemical water splitting on TiO_2 , with potential applications in solar energy conversion, has triggered extensive investigation of water on TiO_2 surfaces, one of the most important materials for photocatalysis and photoelectrochemical cells.^{5–8} A fundamental question on which many studies have focused is whether water adsorption is molecular or dissociative. The existence of OH^- radicals created by water

dissociation can indeed cause dramatic changes to the chemical properties of the surface, as recently discussed, e.g., in ref 9. The question of water adsorption on the rutile (110) surface—the most extensively studied TiO_2 surface—has been especially controversial.⁸ After long debates, it seems now well established that the adsorption is molecular, with dissociation taking place only at defect sites.^{10–15} A similar picture also holds for the (101) surface of the TiO_2 –anatase polymorph,^{16–18} which is the most stable and most frequently exposed surface in anatase nanocrystals. On the other hand, some dissociation has been experimentally observed on rutile $\text{TiO}_2(100)-1 \times 1$,^{19,20} and theoretically predicted on anatase (001).¹⁷

[†] Università degli Studi di Milano-Bicocca.

[‡] Princeton University.

[§] Tulane University.

[⊥] Louisiana State University.

^{||} University of Nebraska.

(1) Thiel, P.; Madey, T. *Surf. Sci. Rep.* **1987**, 7, 211–285.

(2) Henderson, M. A. *Surf. Sci. Rep.* **2002**, 46, 1.

(3) Brown, G. E., Jr.; et al. *Chem. Rev.* **1999**, 99, 77–174.

(4) Brown, G. E., Jr. *Science* **2001**, 294, 67–70.

(5) (a) Hagfeldt, A.; Grätzel, M. *Chem. Rev.* **1995**, 95, 49–68. (b) Grätzel, M. *Nature* **2001**, 414, 338.

(6) Hoffmann, M. R.; Martin, S. T.; Choi, W.; Bahnemann, D. W. *Chem. Rev.* **1995**, 95, 69–96.

(7) Linsebigler, A.; Lu, G.; Yates, J. T. *Chem. Rev.* **1995**, 95, 735–758.

(8) Diebold, U. *Surf. Sci. Rep.* **2003**, 48, 53–229.

(9) Cicero, G.; Catellani A.; Galli G. *Phys. Rev. Lett.* **2004**, 93, 016102.

(10) Henderson, M. A. *Surf. Sci.* **1996**, 355, 151–166.

(11) Hugenschmidt, M. B.; Gamble, L.; Campbell, C. T. *Surf. Sci.* **1994**, 302, 329–340.

(12) Kurtz, R. L.; Stockbauer, R.; Madey, T. E.; Roman, E.; de Segovia, J. L. *Surf. Sci.* **1989**, 218, 178.

(13) Brookes, I. M.; Murny, C. A.; Thornton, G. *Phys. Rev. Lett.* **2001**, 87, 266103.

(14) Schaub, R.; Thostrup, R.; Lopez, N.; Laegsgaard, E.; Stensgaard, I.; Norskov, J. K.; Besenbacher, F. *Phys. Rev. Lett.* **2001**, 87, 266104.

(15) Harris, L. A.; Quong, A. A. *Phys. Rev. Lett.* **2004**, 93, 086105.

(16) Herman, G.; Dohnálek, Z.; Ruzsicky, N.; Diebold, U. *J. Phys. Chem. B* **2003**, 107, 2788.

(17) Vittadini, A.; Selloni, A.; Rotzinger, F.; Grätzel, M. *Phys. Rev. Lett.* **1998**, 81, 2954.

(18) Tilocca, A.; Selloni, A. *J. Phys. Chem. B* **2004**, 108, 4743.

(19) Henderson, M. A. *Langmuir* **1996**, 12, 5093–5098.

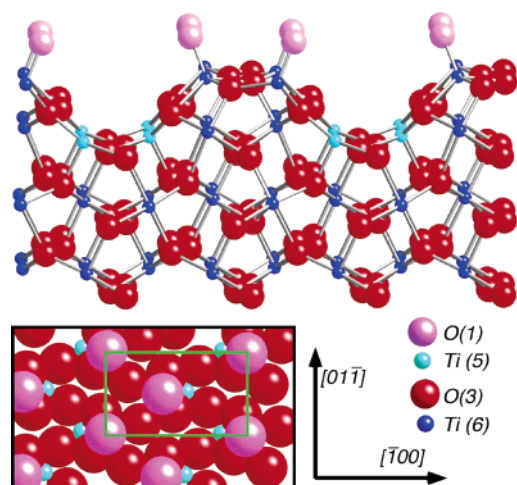


Figure 1. Model of a $\text{TiO}_2(011)$ surface. Upper panel: side view along $[110]$. The top of the slab shows the geometry of the (2×1) reconstruction, the bottom the bulk-terminated (1×1) surface. The coordination of surface atoms is indicated. Lower panel: top view. The (2×1) unit cell is indicated.

The purpose of this paper is to explore the nature of water adsorption on a relatively little investigated TiO_2 surface, namely the (2×1) reconstructed rutile (011) surface. Given the large wealth of available information on water–titania interactions, the interest of studying water adsorption on still another TiO_2 surface may seem rather limited. Instead, there are at least two good reasons for which a study of this type is important. A general reason is that this can help to understand the interaction of water with TiO_2 nanoparticles, which expose different surface terminations and are often grown in an aqueous environment.²¹ In particular, since the rutile (110) and anatase (101) majority surfaces are fairly unreactive, it is likely that the reactivity of titania nanoparticles is dominated by minority surfaces like the one considered here.

A second, more specific reason for studying the rutile (011) surface is that we have recently found that $\text{TiO}_2(011)$ forms a stable (2×1) reconstruction, in which the surface is terminated by doubly bonded $\text{Ti}=\text{O}$ titanyl groups (Figure 1).²² There is at present a considerable interest in such metal–oxygen doubly bonded $\text{M}=\text{O}$ surface species. In addition to the $\text{M}=\text{O}$ species which are “naturally” present, as a result of simple bulk termination, on a few oxide surfaces like $\text{MoO}_3(010)$ and $\text{V}_2\text{O}_5(010)$,²³ recently $\text{M}=\text{O}$ surface groups have been predicted/observed to occur also in materials where no such species are present in the bulk, particularly on the $\text{Cr}_2\text{O}_3(0001)$,²⁴ $\text{V}_2\text{O}_3(0001)$,²⁵ and hematite $\alpha\text{-Fe}_2\text{O}_3(0001)$ ²⁶ surfaces. These results

have led to the suggestion that $\text{M}=\text{O}$ species may be a characteristic structural motif of many surfaces under certain oxygen pressure conditions^{26c} and have stimulated much interest in the influence of these species, e.g., on the surface catalytic activity.

The above observations provide further motivation for our present study. Prior to our investigation of $\text{TiO}_2(011)-(2 \times 1)$,²² double-bonded titanyl groups had been suggested to occur only at the edges of anatase nanoparticles,²⁷ but not on flat titania surfaces. Thus, $\text{Ti}=\text{O}$ species appear to be a unique feature that distinguish the (011) surface from all other known TiO_2 surfaces, and may influence its activity in certain photoelectrochemical experiments. Recent investigations of the dependence of the photocatalytic activity of rutile TiO_2 on the surface orientation indeed indicate that the (011) surface has the highest activity for certain reactions.^{28,29}

To better understand the properties of $\text{TiO}_2(011)-(2 \times 1)$ and the role of surface titanyls, as well as to confirm their existence, in this paper we present a combined experimental and theoretical investigation of water adsorption on stoichiometric and reduced $\text{TiO}_2(011)$ surfaces at different temperatures. We use several experimental techniques, namely ultraviolet photoemission spectroscopy (UPS), scanning tunneling microscopy (STM), and low-energy He^+ ion scattering (LEIS), and compare our results to density functional theory (DFT) calculations for different water coverages. We find that some dissociative adsorption takes place at low water coverage, independent of temperature and for both stoichiometric and reduced surfaces. Support for dissociation is provided by theory, low-temperature UPS, and room-temperature STM measurements. Low-temperature UPS spectra further show that molecular adsorption becomes rapidly dominant with increasing water coverage. Consistent with this observation, calculations predict that a mixed half molecular and half dissociated state is energetically favored at monolayer coverage.

II. Experimental Section

A. Materials and Setup. All experiments were done under ultra-high-vacuum (UHV) conditions with a base pressure below 4×10^{-10} mbar. Polished rutile $\text{TiO}_2(011)$ single crystals were obtained from MTI, Inc. They were cleaned by Ar^+ ion sputtering and annealing cycles with annealing temperatures of 650 °C. The quality of the (2×1) reconstruction was checked by LEED and STM. Water was cleaned by repeated freeze–pump–thaw cycles and dosed by backfilling the UHV chamber through a leak valve. The purity of the water vapor was checked by mass spectrometry.

Low-energy helium ion scattering (LEIS) was accomplished using an ion energy of 1225 eV; a He pressure of 1×10^{-6} mbar gave a sample current of ~ 9 nA. Empty-states scanning tunneling microscopy (STM) images were acquired with positive sample bias voltages. During STM and LEIS measurements, the sample was kept at room temperature.

The UPS experiments described here were performed at the end station of the 3m TGM beam line at the Center for Advanced

(20) Muryn, C. A.; Hardman, P. J.; Crouch, J. J.; Raiker, G. N.; Thornton, G.; Law, D. S. L. *Surf. Sci.* **1991**, *251*, 747–752.

(21) (a) Chemseddine, A.; Moritz, T. *Eur. J. Inorg. Chem.* **1999**, 235–245. (b) Burnside, S. D.; Shklover, V.; Barbé, C.; Comte, P.; Arendse, F.; Brooks, K.; Grätzel, M. *Chem. Mater.* **1998**, *10*, 2419–2425. (c) Gao, Y.; Elder, S. A. *Mater. Lett.* **1999**, *44*, 228–232. (d) Zhang, H.; Finnegan, M.; Banfield, J. F. *Nano Lett.* **2001**, *1*, 81–85.

(22) Beck, T. J.; Klust, A.; Batzill, M.; Diebold, U.; Selloni, A.; Di Valentin, C. *Phys. Rev. Lett.* **2004**, *93*, 036104.

(23) Hermann, K.; Witko, M. In *The Chemical Physics of Solid Surfaces*; Woodruff, D. P., Ed.; Elsevier Science: Boca Raton, FL, 2001; Vol. 9, Oxide Surfaces, pp 136–198.

(24) (a) Dillmann, B.; et al. *Faraday Discuss.* **1996**, *105*, 295–315. (b) Seiferth, O.; Wolter, K.; Dillmann, B.; Klivenyi, G.; Freund, H.-J.; Scarano, D.; Zecchina, A. *Surf. Sci.* **1999**, *421*, 176–190. (c) Wang, X.-G.; Smith, J. R. *Phys. Rev. B* **2003**, *68*, 201402(R).

(25) (a) Dupuis, A.-C.; Abu Hajja, M.; Richter, B.; Kühlenbeck, H.; Freund, H.-J. *Surf. Sci.* **2003**, *539*, 99–112. (b) Schoiswohl, J.; Sock, M.; Surnev, S.; Ramsey, M. G.; Netzer, F. P.; Kresse, G.; Anderse, J. N. *Surf. Sci.* **2004**, *555*, 101–117.

(26) (a) Bergmeyer, W.; Schweiger, H.; Wimmer, E. *Phys. Rev. B* **2004**, *69*, 195409. (b) Rohrbach, A.; Hafner, J.; Kresse, G. *Phys. Rev. B* **2004**, *70*, 125426. (c) Lemire, C.; Bertarione, S.; Zecchina, A.; Scarano, D.; Chaka, A.; Shaikhutdinov, S.; Freund, H.-J. *Phys. Rev. Lett.* **2005**, *94*, 166101.

(27) Rajh, T.; Nedeljkovic, J. M.; Chen, L. X.; Poluektov, O.; Thurnauer, M. C. *J. Phys. Chem. B* **1999**, *103*, 3515–3519.

(28) Rohrer, G. S. In *The Chemical Physics of Solid Surfaces*; Woodruff, D. P., Ed.; Elsevier Science: Boca Raton, FL, 2001; Vol. 9, Oxide Surfaces, pp 485–513.

(29) Wilson, J. N.; Idriss, H. *J. Catal.* **2003**, *214*, 46.

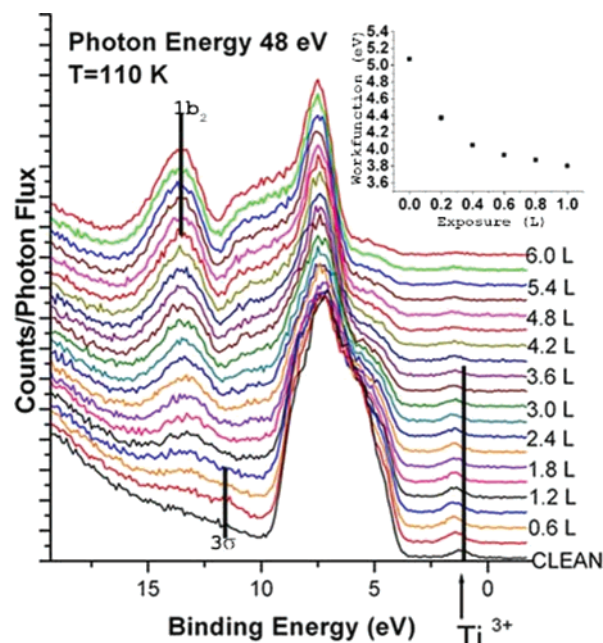


Figure 2. Photoemission spectra of a slightly defective $\text{TiO}_2(011)-(2\times 1)$ after exposing it to 6 L of water in 0.3-L steps at 110 K. The inset shows the work function of the sample with increasing water coverage.

Microstructures and Devices (CAMD) at Louisiana State University. In this setup, sample cooling with liquid nitrogen was accomplished via a cooling rod attached to a solid copper block. The photoelectrons were detected by an angle-resolved hemispherical analyzer with a $\pm 1^\circ$ acceptance angle. An extended description of this setup is available elsewhere.³⁰ Spectra shown in this paper were taken at normal emission. The binding energy scales were calibrated using the Fermi level determined from photoemission of the clean Ta sample plate on which our sample was mounted. Unless noted otherwise, a photon energy of 48 eV was used for obtaining the photoemission data. This photon energy was chosen because it emphasizes photoemission from Ti-derived states through a well-known resonance effect with the Ti 3p states.³¹ It also serves for convenient comparison with previous work on the $\text{TiO}_2(110)$ surface by Kurtz et al.¹² No evidence for photon-induced dissociation was observed during these experiments.^{32,33} The work function of the sample was determined by measuring the low-energy cutoff of the secondary electrons.

B. Low-Temperature Adsorption. Figure 1 shows UPS spectra after incremental exposures to water at 110 K, the lowest temperature reached in our experimental setup. These spectra were taken on a slightly reduced surface; results for a stoichiometric surface are quite similar at this temperature. The intensity of the band-gap state (labeled Ti^{3+} in Figure 2) at 1.2 eV binding energy can be taken as a measure of the nonstoichiometry of the clean TiO_2 surface.⁸ The inset in Figure 2 shows the work function of the sample decreasing with additional exposure to water. This behavior is well reproduced by the DFT calculations (see section IIID).

When dosing water, new states appear below the valence band region. The water-related features can be seen more clearly in the difference spectra in Figure 3. For computation of the difference spectra, all spectra were normalized to give the same count rate in a region below the valence band that contains no water-induced features. The difference spectra were then obtained by subtracting the spectrum of the clean

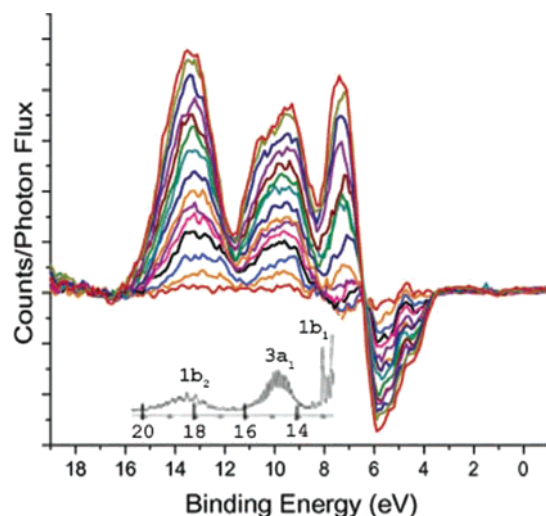


Figure 3. Difference spectra of photoemission spectra shown in Figure 2, taken after water adsorption at 110 K. The inset, taken from Turner et al.,³⁴ shows a photoemission spectrum of water in the gas phase (referenced to the vacuum level). The spectrum has been shifted to compensate for the work function of TiO_2 .

surface from each subsequent spectrum. A gas-phase water photoemission spectrum is inset in Figure 3 and compares remarkably well (after shifting the binding energy to account for the work function of TiO_2) to the difference spectra from the water-covered surface. Consequently, the three features with binding energies of 13.5, 9.8, and 7.4 eV in the difference spectra are attributed to the $1b_2$, $3a_1$, and $1b_1$ states of molecular water, respectively. Their intensity steadily increases with exposure, indicating multilayer adsorption, which is expected at temperatures below 160 K.^{1,2} The $1b_2$ peak narrows with increasing coverage and shifts to slightly higher binding energies, probably because of interactions between the water molecules in the ice layer. In the difference spectra, a negative excursion is visible at the upper edge of the valence band region. This indicates that little, if any, additional states due to interaction with water appear in this region and photoemission from these higher-lying states of the TiO_2 surface are only attenuated by the water overlayer. In our previous work²² we have identified $\text{Ti}=\text{O}$ states of the titanyl groups to be located at the upper edge of the valence band. These can be seen more clearly at lower photon energies; see Figure 1 in the Supporting Information (SI).

Looking in greater detail at the adsorption at low exposures, several features are observed. Two peaks below the valence band become noticeable at 13.2 and 11.4 eV at the lowest coverages; see Figures 2 and 1-SI. On the $\text{TiO}_2(110)$ surface, Kurtz et al. have identified the $1b_2$ feature of molecular water and the 3σ orbital of dissociated water to lie at around 13 and 11 eV, respectively.¹² The binding energy of the 3σ state of OH^- is close to that of the $3a_1$ state of molecular water. However, the relative intensities of the different peaks can be used to determine if dissociated water is present. Note the traces after exposure to 0.3 L of water in Figures 2 and 1-SI. In these spectra, the 3σ OH^- feature at 11.4 eV is higher in intensity than the $1b_2$ state of the molecular water located at 13.2 eV, suggesting the presence of hydroxyls. The presence of a 3σ between the $1b_2$ and the $3a_1$ states gives rise to the broad, smeared-out feature in the lowest trace of the difference spectra in Figure 3. We find indication of dissociated water up to exposures of 0.4 L. Above 0.6 L, the molecular states become too strong, making the identification of the 3σ state difficult. We conclude that at low coverages, and low temperatures, water adsorbs both dissociatively and molecularly on the $(011)-(2\times 1)$ surface.

The behavior of the band-gap state (labeled Ti^{3+} in Figures 2 and 1-SI) is interesting. On a clean sample, this peak indicates the presence of surface oxygen vacancies. Remarkably, we find that this peak increases in intensity with water dosage, with maximum intensity

(30) Dowben, P. A.; Lagraffe, D.; Onellion M. *J. Phys.: Condens. Matter* **1989**, *1*, 6571–6587.

(31) Bertel, E.; Stockbauer, R.; Madey, T. E. *Surf. Sci.* **1984**, *141*, 355–387.

(32) Weissenrieder, J.; Mikkelsen, A.; Anderson, J. N.; Feibelman, P. J.; Held, G. *Phys. Rev. Lett.* **2004**, *93*, 196102.

(33) Andersson, K.; Nikitin, A.; Pettersson, L. G. M.; Nilsson A.; Ogasawara, H. *Phys. Rev. Lett.* **2004**, *93*, 196101.

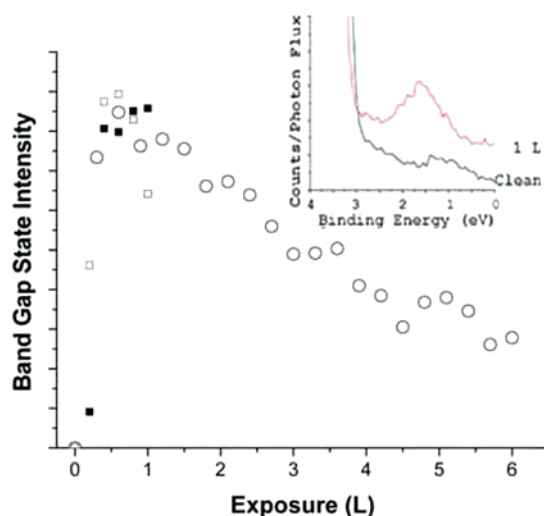


Figure 4. Intensity of the band gap state (labeled Ti^{3+} in Figures 2 and 1-SI) with increasing water coverage. The different symbols represent gap state intensities from different experiments. The inset shows spectra of the band gap region taken from a clean, nearly perfect sample and after dosing with 1 L of water.

around 1 L; see Figure 4. We have repeated the experiment with different levels of defect densities. The increase in intensity and the maximum value appear to be independent of the number of gap states present on the clean sample before the water exposure. The Ti^{3+} state also shifts to 0.3 eV higher binding energy at the lowest water exposures. Higher water dosages do not affect the position of the state any further.

A somewhat similar behavior of the band gap state has been observed in photoemission experiments by Kurtz et al.¹² on $\text{TiO}_2(110)$: when nearly perfect surfaces were dosed with massive amounts of water at room temperature, the appearance of a band gap state was observed. On slightly reduced surfaces, where water binds dissociatively to oxygen vacancies, the intensity of the band gap state was not suppressed by the formation of hydroxyls. Similarly, the Ti^{3+} state in XPS is not quenched by dosing water.³⁵

A possible explanation of these previous and our present results could be that the (shifted) Ti^{3+} state is related to the presence of hydroxyls at the surface. This would explain why the Ti^{3+} state is not attenuated in photoemission experiments, although oxygen vacancies are clearly covered with hydroxyls. It also helps to rationalize the shift in the Ti^{3+} state in Figures 2 and 1-SI, which happens simultaneously with the appearance of the 3σ state. Probably, surface defects are immediately filled with dissociated water. Thus, the Ti^{3+} state, which is indicative for oxygen vacancies on the slightly reduced, clean surface, rigidly shifts to the position related to the hydroxyl groups. If one adopts such an OH-related Ti^{3+} state in the band gap, the results in Figure 4 allow an interesting conclusion regarding the composition of the first layer of water: the Ti^{3+} increases with coverage up to an exposure of 1 L, indicating that dissociated water is continuously formed up to the point where the surface is completely covered with a layer of water. Further water exposure leads to the formation of multilayers and an attenuation of the gap state in photoemission. Thus, the Ti^{3+} state may represent a much more sensitive measure of hydroxylation than the molecular peaks that are usually invoked to assign the state of adsorbed water on surfaces. It is difficult to quantify the percentage of dissociated water within the first layer. However, on the basis of a comparison of our spectra with ones of Kurtz et al.¹² (both data have been taken under similar experimental conditions), an approximate value of at least 20% can be estimated.

(34) Turner, D. W.; Baker, C.; Baker, A. D.; Brundle, C. R. *Molecular Photoelectron Spectroscopy*; Wiley-Interscience: New York, 1970.

(35) Pan, J. M.; Machhoff, B. L.; Diebold, U.; Madey, T. E. *J. Vac. Sci. Technol.* **1992**, *10*, 2470.

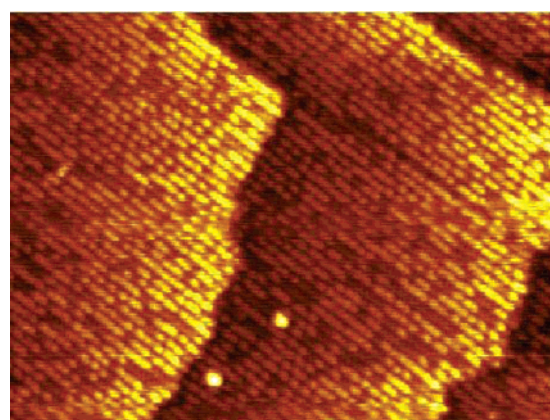


Figure 5. Constant current STM image ($40 \times 30 \text{ nm}^2$, $V_{\text{sample}} = +1.2 \text{ V}$ and $I_{\text{tunnel}} = 0.5 \text{ nA}$) of TiO_2 after exposure to water vapor at room temperature.

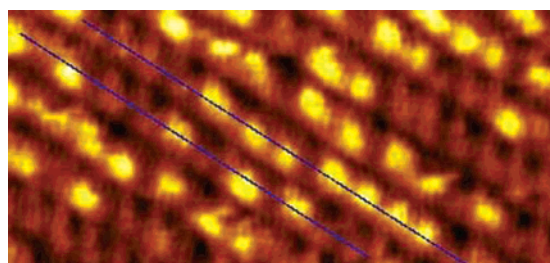


Figure 6. Constant current STM image ($8 \times 4 \text{ nm}^2$, $U_{\text{bias}} = 1.2 \text{ V}$, $I = 0.5 \text{ nA}$) of TiO_2 after exposure to 5 L of water vapor at room temperature. The lines mark the center of the zigzag rows of the (2×1) reconstruction.

While the computational results of the electronic density of states (DOS) in section IIIE generally agree quite well with the photoemission spectra, they do not show the splitting-off of a gap state when dissociated water is present. Hence, the origin of an OH-related gap state has to remain somewhat speculative. Recent results by Henderson et al.³⁶ point toward a possible explanation, however. These authors observed that UV irradiation of an organic overlayer on $\text{TiO}_2(110)$ led to the formation of a Ti^{3+} state. They assigned this state to the trapping of a photo-excited electron at the interface between the surface and the overlayer. Possibly, the UV light used in our photoemission experiment also creates excited electrons that are trapped at hydroxyls at the surface.

C. Adsorption at Room Temperature. Figure 5 shows an empty-states STM image of the $\text{TiO}_2(011)$ surface exposed to 5 L of water at room temperature. Bright rows along the $[011]$ direction in empty-states STM images correspond to the titanyl rows on the clean $\text{TiO}_2(011)-(2 \times 1)$ surface.²² Dense lines of bright water-induced features are observed on these rows. It is widely accepted that water molecules adsorb on under-coordinated metal atoms on metal oxides.^{2,8} The only under-coordinated Ti atoms on the $\text{TiO}_2(011)-(2 \times 1)$ surface are the five-fold-coordinated $[\text{Ti}(5)]$, located in the troughs between the titanyl rows.²² The water-induced bright spots on the rows observed by STM are located on top of the bright rows of the substrate, suggesting that these are hydrogen atoms located on the titanyl groups. Calculated STM images using the Tersoff–Haman approximation³⁷ confirm this assignment; see section IIIF. The calculations also confirm that water molecules or hydroxyl groups adsorbed in the troughs of the $\text{TiO}_2(011)-(2 \times 1)$ reconstruction are invisible in the STM images due to geometrical height differences.

Figure 6 shows a high-resolution STM image of $\text{TiO}_2(011)$ after exposure to 5 L of water at room temperature. In addition to the zigzag

(36) Henderson, M. A.; White, J. M.; Uetsuka, H.; Onishi, H. *J. Am. Chem. Soc.* **2003**, *125*, 14974.

(37) Tersoff, J.; Hamann, D. R. *Phys. Rev. Lett.* **1983**, *50*, 1998.

rows formed by the titanyl groups, bright features can be seen on these rows. These features are not present on the clean surface. The position of these bright spots is slightly off from the center of the zigzag rows, which is marked in Figure 6. From this we conclude that the bright spots correspond to atoms adsorbed on the titanyl oxygens. Furthermore, if a titanyl group on one side of the zigzag row is occupied by an adsorbate, this adsorbate seems to block adsorption at the neighboring titanyl groups on the other side of the zigzag row. The adsorbates also have the tendency to form short lines along the $[011]$ direction (parallel to the zigzag rows), covering only one side of the zigzag.

The density of the water-induced features seems to saturate after exposures above 5 or 6 L of water. At this exposure, about 30% of the titanyl groups are covered with adsorbates. Temperature-dependent photoemission spectra were taken on the surface during adsorption and desorption. Molecular features disappear around 200 K, and dissociated water remains on the surface up to temperatures close to 300 K. Further confirmation of water adsorption at room temperature comes from low-energy ion scattering spectroscopy (LEIS); see the Supporting Information.

Summarizing, our experimental results suggest that water adsorbs mostly molecularly at low temperatures, with indications for dissociative adsorption within the first monolayer. At room temperature water adsorbs only dissociatively, and the amount of dissociation appears to be independent of the oxidation state of the surface. The significant amount of hydroxylated titanyl groups found in the STM images suggests that the perfect $\text{TiO}_2(011)-(2 \times 1)$ surface is active with respect to water dissociation. Furthermore, STM shows a short-range order of the dissociation products. The theoretical results discussed in the next section support these observations and give further insight into the adsorption process.

III. Theoretical Section

A. Calculation Details. The calculations have been performed using the plane-wave-pseudopotential approach, together with the Perdew–Burke–Ernzerhof (PBE)³⁸ exchange–correlation functional and ultrasoft pseudopotentials³⁹ (with kinetic energy cutoffs of 25 and 200 Ry for the smooth part of the electronic wave functions and augmented electron density, respectively). We used the ESPRESSO package⁴¹ including the CP90 and PWSCF codes: CP90, based on the Car–Parrinello (CP) approach,⁴⁰ was employed for geometry optimizations and molecular dynamics (MD), limiting the Brillouin zone sampling to the Γ point, while the PWSCF code⁴¹ was used to perform calculations at a low-symmetry k -point and obtain projected density of states and STM images.

For the surface structure, we considered our recently proposed (2×1) reconstruction model,²² shown in Figure 1. The supercell comprised two (2×1) surface cells. The optimized bulk lattice parameters are taken from previous calculations, which were performed using the same approximations as in this work.⁴² Slab models with both four and six Ti layers were used. Except for the lowest layer atoms, which were kept fixed in their bulk positions, all atoms were allowed to relax using a second-order damped dynamics until all components of the residual forces were less than 0.025 eV/Å. The use of thicker slabs was found to improve the relative surface energy of the reconstructed (2×1) $\text{TiO}_2(011)$ surface, allowing long-range relaxation of the lattice.

(38) Perdew, J. P.; Burke, K.; Ernzerhof, M. *Phys. Rev. Lett.* **1996**, 77, 3865–3868.

(39) Vanderbilt, D. *Phys. Rev. B* **1990**, 41, 7892.

(40) Car, R.; Parrinello, M. *Phys. Rev. Lett.* **1985**, 55, 2471.

(41) Baroni, S.; dal Corso, A.; de Gironcoli, S.; Ghanzori, P.; Cavazzoni, C.; Ballabio, G.; Scandolo, S.; Chiarotti, G.; Focher, P.; Pasquarello, A.; Laasonen, K.; Trave, A.; Car, R.; Marzari, N.; Kokalj, A., <http://www.pwscf.org>.

(42) Lazzeri, M.; Vittadini, A.; Selloni, A. *Phys. Rev. B* **2001**, 63, 155409.

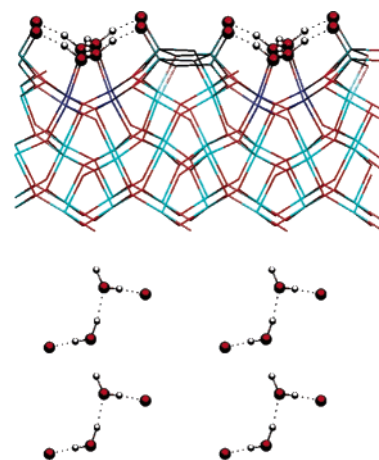


Figure 7. Calculated structure of 1 ML of water adsorbed on the (2×1) reconstructed $\text{TiO}_2(011)$ surface: (fully) molecular state. Upper panel, side view; lower panel, top view of the uppermost layer of O and H atoms.

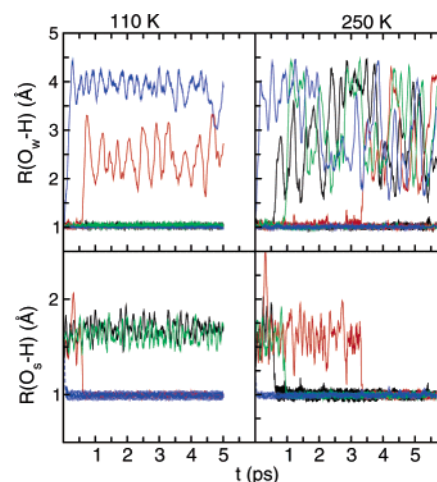


Figure 8. Time evolution of selected interatomic distances along the MD simulations. Left panels, 110 K; right panels, 250 K. $R(\text{O}_w\text{--H})$ is the distance between water oxygen and its two protons for each molecule. $R(\text{O}_s\text{--H})$ is the distance between titanyl oxygens and the closest hydrogen.

Car–Parrinello⁴⁰ molecular dynamics simulations at full monolayer (ML) coverage were carried out at two different temperatures, namely 110 and 250 K, using a four-layer-thick slab comprising two (2×1) surface cells. The time step δt and the fictitious electronic mass μ were fixed at 0.145 fs and 700 au, respectively; the deuterium mass was used for hydrogen atoms, to allow for larger μ and δt .

B. Molecular Dynamics Simulations. The starting configuration for the Car–Parrinello⁴⁰ MD simulations was a (locally optimized) structure with a full molecular water layer (four molecules) adsorbed on the five-fold-coordinated Ti atoms of the structural model in Figure 1 (see Figure 7). The total length of each simulation was about 5 ps (35 000 steps).

The time evolution of selected interatomic distances, shown in Figure 8, provides a clear picture of the events occurring along the dynamics. At 110 K, one water molecule transfers a proton to a titanyl group almost immediately: see the increase in an $\text{O}_w\text{--H}$ distance and the decrease in the corresponding $\text{O}_s\text{--H}$ distance (blue curves in the left panels of Figure 8), where O_w and O_s are the water and titanyl oxygen atoms, respectively. A second water molecule (red curves) dissociates after less than a picosecond. This mixed molecular–dissociated monolayer (see

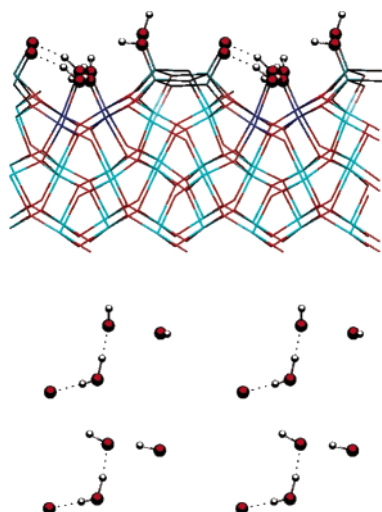


Figure 9. Calculated structure of 1 ML of water adsorbed on the (2×1) reconstructed TiO₂(011) surface: mixed (molecular and dissociated) state. Upper panel, side view; lower panel, top view of the uppermost layer of O and H atoms.

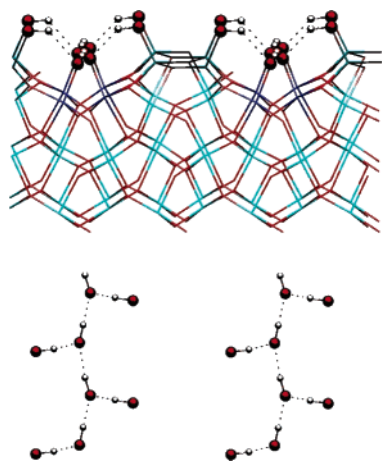


Figure 10. Calculated structure of 1 ML of water adsorbed on the (2×1) reconstructed TiO₂(011) surface: (fully) dissociated state. Upper panel, side view; lower panel, top view of the uppermost layer of O and H atoms.

Figure 9) is stable in the remaining 4 ps of the 110 K trajectory, with no further dissociations or recombinations.

At 250 K, we observe again two dissociations in the first picosecond, this time followed by two more dissociations at 1 and 3.5 ps. Therefore, a full dissociated monolayer (Figure 10) is formed at 250 K, which appears to be stable for the remaining 2 ps (Figure 8, right panels).

Thus, these MD simulations indicate a high reactivity of the surface toward water dissociation. A first intermediate state with a mixed dissociated and molecular water layer is formed and is stable at 110 K, whereas it can be further transformed into a full dissociated layer at 250 K. Although no water desorption was observed in both 110 and 250 K MD simulations, we cannot rule out the possibility of desorption on a longer time scale.

The time evolution of the distances shown in Figure 8 (and a direct inspection of the MD trajectories) shows the presence of two different orientations for the O_s–H hydroxyl: the H atom can point toward the original O_w, forming a weak hydrogen bond with $R(\text{O}_w\text{--H}) \approx 2.5$ Å, or it can point away from it (along [100]), with $R(\text{O}_w\text{--H}) \approx 4$ Å. These orientations are “frozen” in the mixed monolayer formed at 110 K, while the much larger

Table 1. Absolute (E_{ads}) and Relative (E_{rel}) Adsorption Energies Per Molecule, and Relative Total Energies per (2×2) Supercell (Δ_{cell})^a

	$\Theta = 0.25$ ML			$\Theta = 1$ ML		
	E_{ads}	E_{rel}	Δ_{cell}	E_{ads}	E_{rel}	Δ_{cell}
Mol	−1.097	0	0	−1.056	0	0
Diss	−1.274	−0.177	−0.177	−1.098	−0.042	−0.168
Mix				−1.121	−0.065	−0.260

^a All values are in eV. Labels Mol, Diss, and Mix denote molecular, dissociative, and mixed adsorption, respectively. Θ Denotes the Water Coverage

rotational freedom about the Ti–O_s(–H) axis at 250 K leads to frequent jumps between them for each of the four hydroxyls. This behavior suggests the existence of a small energy barrier (between 1 and 2 kJ mol^{−1}) for the rotation along the Ti–O_s(–H) axis, which can be overcome frequently at 250 K, but not at the lower temperature.

In the fully dissociated ML, all one-fold oxygens are protonated, so that both sides of the zigzag chain formed by the titanyl groups host O_sH groups. On the other hand, the O_sH groups in the mixed monolayer (Figure 9) are formed on the same side of the zigzag chain of titanyls, and the opposite side is devoid of protons, similarly to the STM results discussed above. This suggests a higher stability of conformations with rows of O_sH aligned on the same side of the zigzag chains. To check this, we considered an alternate mixed-monolayer structure in which two O_sH groups were located on opposite sides of the chain. This structure turns out to be 0.14 eV less stable than the structure in Figure 9. Moreover, if a short MD trajectory at 110 K is started from it, an immediate recombination is observed, where an O_sH proton is transferred back to an O_wH in the valley, followed by dissociation of another water molecule to form the more stable mixed ML with O_sH groups on the same side of the zigzag chain. This confirms the low stability of the initial structure.

C. Total Energy Calculations. Full geometry optimizations were performed for molecular, dissociated, and mixed ML configurations (see Figures 7, 9 and 10, respectively) using a six-layers-thick slab. For the mixed monolayer we used the configuration obtained from the 110 K MD simulation described above. In this configuration the O_sH groups are either pointing upward (‘up’, upper part of the top view in Figure 9) or toward the O_wH, forming a hydrogen bond (‘down’, bottom part of the top view in Figure 9). Further optimization at a low-symmetry k -point was also performed in order to improve the sampling of the Brillouin zone. Adsorption energies, calculated with respect to the energies of the separated substrate and adsorbate, are reported in Table 1.

At full ML coverage the mixed molecular + dissociative configuration has the largest adsorption energy (−1.121 eV), while molecular adsorption is characterized by the smallest energy value (−1.056 eV). This energetics computed at 0 K is consistent with what is observed during the MD runs: since at low temperature (110 K) the enthalpic term is dominant, the mixed layer is the stable configuration, while at high temperature (250 K), when the entropic term becomes more relevant, dissociation of all water molecules on the surface is expected. This agrees well with the experimental results, which indicate a partially dissociated layer at low temperatures and complete dissociation at room temperature. It is interesting to note that

at high coverage a variety of intermolecular hydrogen bonds is formed between both molecular and dissociated species. These bonds are highly directional and therefore may lead to the stabilization of special configurations, especially in the case of the mixed-type adsorption.

At 25% coverage, corresponding to one adsorbed water molecule per supercell (see Figure 12, below), the dissociated form is more stable than the molecular one by 0.18 eV. Given the low density of water molecules present on the surface, the number of hydrogen bonds formed is negligible. Experimentally, the fully dissociated layer is not seen at low coverages and temperatures in the photoemission experiments. This, however, is not surprising: water molecules are known to exhibit a strongly attractive interaction,¹ which can lead to the formation of two-dimensional clusters, as has been observed on another oxide.⁴³ So even if the total coverage is far less than a monolayer, the *local* coverage can be much higher and only a mixed layer will be observed in the experiment.

D. Work Function. The work function (Φ) has been calculated from the electrostatic potential profile along the slab (see, e.g., ref 44), using $\Phi = E_{\text{vac}} - E_{\text{c}}$, where E_{vac} is the electrostatic potential energy in the vacuum region and E_{c} the bottom of the conduction band in the slab. E_{c} has been chosen as a reference energy because this is where the Fermi energy is located in the experimental samples. For these calculations, slabs of six layers have been considered; water molecules were all dissociated at 0.5 ML coverage, whereas the mixed, half molecular and half dissociated, configuration was taken at 1 ML coverage. In this way we obtain $\Phi = 5.7, 4.8$, and 4.4 eV for water coverages of 0, 0.5, and 1 ML, respectively. The calculated values appear to be larger than the experimental ones in Figure 2, which may be due to the DFT underestimate of the band gap (2.3 eV in our calculations). In spite of this, the calculations very well describe the experimental trend of decreasing work function with increasing water coverage, from 5.1 eV for the clean surface to 3.8 eV after exposure to 1 L of water. It is noteworthy that this experimental trend is not well reproduced if the work function is calculated for either a fully molecular or a fully dissociated water monolayer, for which we find $\Phi = 5.2$ and 4.7 eV, respectively.

E. Density of States. Figure 11 shows the electronic densities of states (DOS) together with selected contributions of oxygen species to the $\text{O}(2p)$ valence band for 0.25 and 1 ML water coverages. At 1 ML coverage, fully molecular, fully dissociated, and mixed monolayers are considered. For 0.25 ML coverage of dissociated water (panel 1), the titanyl oxygens give rise to a well-defined peak at the upper edge of the valence band (green line), whereas the O atoms in the hydroxyl groups resulting from dissociation of a water molecule (O_{wH} , adsorbed on the five-fold-coordinated $\text{Ti}(5)$ sites, and O_{sH} , resulting from protonation of the titanyl oxygen, blue and red lines, respectively) give rise to two almost overlapping peaks at the lower edge of the valence band (3σ states) and to another broader feature in the middle of the valence band (1π state).

For the fully dissociated monolayer, in the second panel of Figure 11, the small peak below the valence band can be assigned to the O_{wH} species (blue line), while the O_{sH} species

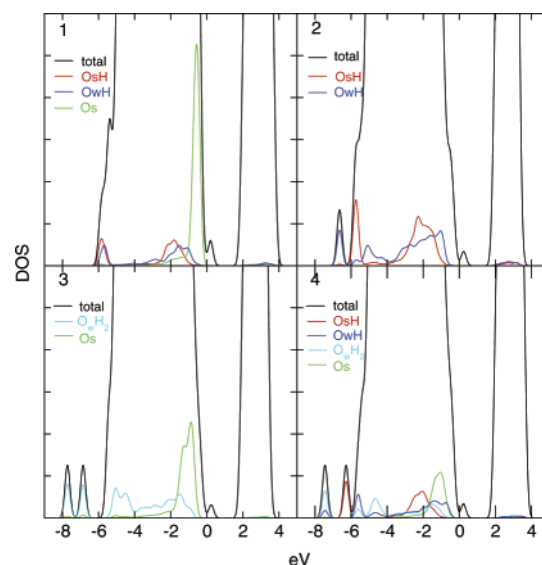


Figure 11. Total DOS and projected DOS on selected O species for different coverages and structural models of water adsorbed on $\text{TiO}_2(011)-(2\times 1)$. Panel 1, 0.25 ML of dissociated water; panel 2, 1 ML of dissociated water; panel 3, 1 ML of molecular water; panel 4, 1 ML of mixed molecular and dissociated water. The energy zero is at the top of the valence band, and the small feature just above it arises from oxygen atoms of the lower, unrelaxed surface of the slab.

produce the peak at the bottom of the valence band (red line), which is essentially at the same position as the corresponding peak for 0.25 ML coverage (panel 1, red line). The splitting in binding energy of these two species is related to the fact that chains of hydrogen-bonded O_{wH} groups are formed along the valleys in the $[01\bar{1}]$ direction (Figure 10). Each of these O_{wH} groups acts simultaneously as an H donor to one neighboring O_{wH} group and as an H acceptor to the other neighbor. Also, the O_{sH} species interact, through weaker hydrogen bonds, with the chain-forming O_{wH} groups in the valleys. The O_{sH} species, however, behave only as proton donors. The large stabilization deriving from formation of the hydrogen-bonded chains may be the reason why the peak related to the O_{wH} species, separating from the valence band, is lower in energy than both the peak of O_{sH} species and that of the corresponding O_{wH} species at 0.25 ML coverage. A splitting of photoemission states has indeed been observed for other systems.⁴⁵ The photoemission peaks in the present study are too broad to allow us to identify a splitting.

Comparison between the total DOS for the surface with 0.25 and 1 ML of dissociatively adsorbed water and the total DOS of the clean surface (see Figure 3 of the Supporting Information) shows that, concomitant with the increasing hydroxylation of the titanyl oxygens, a small peak appears below the valence band and the peak at the upper edge of the valence band disappears. As discussed above, the 3σ peak is strongly coverage-dependent and is almost degenerate with the valence band for the low-coverage case.

In the third panel of Figure 11, the total and projected density of states for 1 ML of molecular water adsorbed on the $\text{Ti}(5)$ is reported. The most evident features are two small peaks below the valence band. These features are due to the oxygens of the water molecules. The peaks are split because the water

(43) Meyer, B.; Marx, D.; Dulub, O.; Diebold U.; Kunat, M.; Langenberg; Wöll, C. *Angew. Chem. Int. Ed.* **2004**, *43*, 6641–6645.

(44) Fall, C. J.; Bingeli, N.; Badereschi, A. *J. Phys.: Condens. Matter* **1999**, *11*, 2689–2696.

(45) Pache, T.; Steinrück, H. P.; Huber, W.; Menzel, D. *Surf. Sci.* **1989**, *224*, 195–214.

molecules tend to form dimers in the limited supercell which has been used for the calculations; see Figure 7. Within these dimers, one of the molecules behaves as proton donor and the other as proton acceptor. In a less ordered situation, the low-energy peaks tend to merge into a single broad feature, centered around the $1b_2$ state of molecular water. The other two broad features in panel 3 of Figure 11 correspond to the contribution of the water O atoms to the valence band and are assigned to the $3a_1$ and $1b_1$ states of molecular water.

In the fourth panel of Figure 11, the total and projected density of states for 1 ML of mixed molecular and dissociated water molecules is presented. The optimized structure of this configuration (Figure 9) is quite complex: dissociated and molecular water species alternate on the Ti(5) sites in the valleys; each undissociated water molecule establishes two hydrogen bonds with the O atom of the neighboring titanyl group and with the O_wH on the next Ti(5), respectively. The projected density of states that results from this complex situation is quite involved. The small peak below the valence band, at ~ -7.6 eV, is attributed to the $1b_2$ state of molecular water (light blue line), with a small contribution also from the O_wH (blue line). The other small peak below the valence band, at ~ -6.4 eV, is attributed to the 3σ state of O_sH species (red line). The $3a_1$ state of undissociated water molecules is in the lower half of the valence band, while the $1b_1$ state of undissociated and 1π state of dissociated species are located in the upper part of the valence band.

F. STM Images. The experimental high-resolution STM image in Figure 6, taken after exposure to a high dosage water vapor at room temperature, indicates that about 30% of the titanyl groups are covered with adsorbates. On the basis of our molecular dynamics simulations, we expect that at this temperature water molecules on the surface are adsorbed in the dissociated form. Thus, empty-state STM images, calculated³⁷ for 0.25 ML coverage of dissociated molecules, should be well suited for comparison with the experimental image. (Calculated images for the mixed water monolayer model are presented in the Supporting Information.)

In the calculated image (see Figure 12), the dominant features originate from the OH groups formed after proton transfer from the water molecules adsorbed on Ti(5) to the surface titanyl oxygens, O_s . However, a weaker feature due to the bare O_s atoms is also evident. In contrast, O_wH groups are not detectable, probably because they lie at a lower level in the valleys. On the basis of these results, we can conclude that the bright spots observed in the experimental image are due to highly protruding O_sH species and the darker zigzag patterned spots are due to the bare O_s atoms, as previously observed for the clean reconstructed surface.

IV. Discussion

From comparative studies of water adsorption on $TiO_2(110)$ and $TiO_2(100)$,¹⁹ it has been concluded that the relative proximity between Ti(5) and under-coordinated surface oxygen atoms is a critical factor in predicting whether a TiO_2 surface will catalyze water dissociation. If the distance between the oxygen atom of the water molecule, bound to a Ti(5) atom, and a neighboring undercoordinated oxygen atom is small, the hydrogen bond between the O_s and the water molecule will be strong enough to result in dissociation. Dissociative adsorption

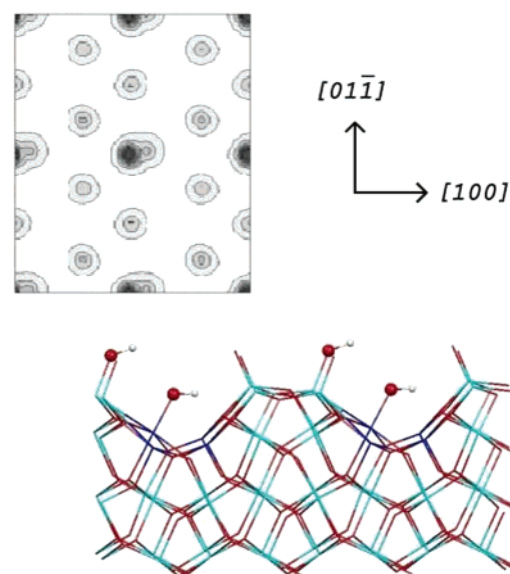


Figure 12. Model for 0.25 ML of dissociated water adsorbed on the 2×1 reconstructed $TiO_2(011)$ surface. Upper panel: calculated STM image in a plane 2.7 Å above the outermost Ti atoms, obtained by integrating the electronic density for empty states within a 1.2 eV window above the conduction band edge. Lower panel: side view of the optimized structure along $[01\bar{1}]$.

has convincingly been shown to occur on $TiO_2(100)-(1 \times 1)$.^{19,20} On $TiO_2(110)$, in contrast, the O_w-O_s distance allows only weak H-bonds to form (with $R(O_w-O_s) = 2.81$ Å), and experimental^{10–12} as well as the latest theoretical results¹⁵ point toward molecular adsorption, except at defects. Applying this simple rule to the case of $TiO_2(011)-(2 \times 1)$ lets one expect dissociation: the O_w-O_s distance is only ~ 2.6 Å, at the borderline between “intermediate” and “strong” H-bonding according to the classification given by Thiel and Madey.¹ In addition, the O_s atoms on $TiO_2(011)-(2 \times 1)$ are bound to only one Ti atom. Such O(1) atoms could act as a stronger Brønsted base than the O(2) atoms that are present on all other TiO_2 surfaces, making the $TiO_2(011)-(2 \times 1)$ surface particularly reactive for water dissociation.

These simple considerations agree well with our experimental and theoretical findings of dissociative water adsorption at low coverages and high temperatures. At monolayer coverage and low temperature, on the other hand, intermolecular hydrogen-bond interactions stabilize a *mixed* layer, according to our total-energy calculations and low-temperature MD simulations. For the $TiO_2(110)$ surface, the formation of such a mixed layer has been proposed,⁴⁶ and hotly debated^{13–15} in the computational literature, yet it has not been observed experimentally. The experimental results in this work strongly support the formation of such a mixed layer on $TiO_2(011)-(2 \times 1)$. The photoemission results point toward the presence of an OH 3σ state at low coverages (see Figures 2 and 1-SI), in addition to the $1b_2$ state of molecular water. As outlined above, a very sensitive measure of the presence of hydroxyls is the formation of a (shifted) band gap state. This state increases in intensity with water exposures and, at 1 L, reaches a maximum that is largely independent of the reduction state of the sample. Given the fact that water on TiO_2 has a unity sticking

(46) Lindan, P. J. D.; Harrison, M. D.; Gillan, M. J. *Phys. Rev. Lett.* **1998**, *80*, 762.

coefficient,⁴⁷ this suggests that hydroxyls are continuously being formed, up to the point where growth of a second layer of water begins.

The number and the position of the hydroxyl groups in the room-temperature STM images point to an interesting scenario: water/surface interaction at the molecular scale. Even at the highest coverage, only 30% of the surface is hydroxylated, and the H atoms on the O_s atoms appear to be located on one side of the zigzag only. The MD simulations show that hydroxyl groups in the mixed layer are stable when located on the same side of the zigzag (Figure 9), while they recombine when placed on opposite sides of the zigzag at 110 K. The low stability of the configuration with opposing hydroxyls is likely related to local strain. The formation of an O_sH hydroxyl locally induces significant modifications of the structure. In particular, the original $\text{Ti}=\text{O}$ double bond becomes ~ 0.2 Å longer, and correspondingly the Ti atom tends to form tighter bonds with the other oxygens to which it is coordinated. This structural deformation extends to the closer atoms on the other side of the zigzag chain, thereby modifying their reactivity, whereas the atoms on the same side of the chain, at larger distance, are unaffected.

Possibly, something similar happens during water adsorption at room temperature: molecular water is temporarily trapped and desorbs again,⁴⁷ unless it is dissociated through interaction with the titanyl oxygen atoms. This can only happen at one side of the titanyl zigzag; once one side is hydroxylated, the other side becomes inactive for dissociation. Temperature-dependent UPS measurements show that, around 200 K, the water molecules of the mixed layer desorb rather than dissociate. This supports our conjecture that only part of the surface is active for dissociation.

Finally, we comment on the potential role of the surface titanyl groups in photocatalysis. As pointed out in the Introduction, the (011) surface of rutile is especially active for some photocatalytic reactions, and in a previous publication²² we conjectured that the surface titanyl groups that are specific to this face might be responsible for some of the observed effects. In section IIB, we further speculate that the Ti^{3+} state in the photoemission spectra is indicative of photo-excited electrons, trapped at OH sites. While efficient trapping of electrons is beneficial for reduction reactions, it is unfavorable for photo-oxidation, as the accumulating charge on the surface causes a rapid quenching of photo-excited holes that migrate to the surface. However, the picture developed in this paper is

consistent with the increased activity for conversion of Ag^+ to metallic Ag that was observed on polycrystalline samples.²⁸

V. Summary and Conclusion

In this paper we have reported on a combined experimental and theoretical study of water adsorption on the reconstructed $\text{TiO}_2(011)-(2\times 1)$ surface, whose structure we have recently described in terms of a model characterized by the presence of one-fold-coordinated oxygens; see Figure 1.²² The present results provide evidence of a complex behavior for adsorbed water, where dissociated and mixed dissociated–molecular adsorption states are thermodynamically favored at low and monolayer coverages, respectively, whereas the adsorption is purely molecular above one monolayer. It should be noted that calculations tend to yield a somewhat larger fraction of dissociated water with respect to that found in experiments, where this fraction does not exceed 30% of a monolayer (against 50% given by calculations). At low temperatures this could be due to the presence of a kinetic barrier hindering dissociation or, as discussed previously, of two-dimensional clustering in the experiment, whereas at room temperature some desorption (not included in the calculations) could take place. Apart from these differences, however, the agreement between our theoretical and experimental results is generally good. Since our computational results are based on the titanyl model of Figure 1, this agreement provides further support to the existence of $\text{Ti}=\text{O}$ double bonds at the surface of the (2×1) reconstructed rutile (011) surface.

Acknowledgment. We thank H.-J. Freund for useful discussion and for pointing out refs 24 and 26. This work has been partially supported by NSF (CHE-0121432 and CHE-010908), the Petroleum Research Fund (PRF #40919-AC5), and NASA. The calculations were performed on the Lemieux Terascale Computing System at the Pittsburgh Supercomputer Center, the IBM-SP3 computer at the Keck Computational Materials Science Laboratory in Princeton, and the Cadillac Linux cluster at the Princeton Institute for Computational Science and Engineering.

Supporting Information Available: Complete refs 3 and 24a; photoemission spectra of $\text{TiO}_2-(2\times 1)$ after incremental water dosages at 110 K, obtained with photon energy of 26 eV; low-energy He ion scattering spectra; comparison of calculated densities of states for 0.25 and 1 ML water coverages; and simulated empty states STM image for the mixed water monolayer model. This material is available free of charge via the Internet at <http://pubs.acs.org>.

(47) Brinkley, D.; Dietrich, M.; Engel, T.; Farrall, P.; Gantner, G.; Schafer, A.; Szumacher, A. *Surf. Sci.* **1998**, 395, 292–306.